Particle tracking stereomicroscopy in optical tweezers: Control of trap shape

Richard Bowman*, **Graham Gibson, and Miles Padgett**

Department of Physics and Astronomy, SUPA, University of Glasgow, G12 8QQ, UK

**r.bowman@physics.gla.ac.uk*

http://www.physics.gla.ac.uk/Optics/

Abstract: We present an optical system capable of generating stereoscopic images to track trapped particles in three dimensions. Two-dimensional particle tracking on each image yields three dimensional position information. Our approach allows the use of a high numerical aperture (NA= 1.3) objective and large separation angle, such that particles can be tracked axially with resolution of 3 nm at 340 Hz. Spatial Light Modulators (SLMs), the diffractive elements used to steer and split laser beams in Holographic Optical Tweezers, are also capable of more general operations. We use one here to vary the ratio of lateral to axial trap stiffness by changing the shape of the beam at the back aperture of the microscope objective. Beams which concentrate their optical power at the extremes of the back aperture give rise to much more efficient axial trapping. The flexibility of using an SLM allows us to create multiple traps with different shapes.

OCIS codes: (140.7010) Laser trapping; (230.6120) Spatial light modulators; (120.4640) Optical instruments; (350.4855) Optical tweezers or optical manipulation.

References and links

1. A. Ashkin, J. M. Dziedzic, J. E. Bjorkholm, and S. Chu, "Observation of a single-beam gradient force optical trap for dielectric particles," Opt. Lett. **11**, 288–290 (1986).
2. M. Reicherter, T. Haist, E. Wagemann, and H. Tiziani, "Optical particle trapping with computer-generated holograms written on a liquid-crystal display," Opt. Lett. **24**, 608–610 (1999).
3. D. G. Grier, "A revolution in optical manipulation," Nature **424**, 810–816 (2003).
4. P. Rodrigo, V. Daria, and J. Glückstad, "Four-dimensional optical manipulation of colloidal particles," Appl. Phys. Lett. **86**, 074103 (2005).
5. G. Sinclair, P. Jordan, J. Courtial, M. Padgett, J. Cooper, and Z. Laczik, "Assembly of 3-dimensional structures using programmable holographic optical tweezers," Opt. Express **12**, 5475–5480 (2004).
6. J. Leach, K. Wulff, G. Sinclair, P. Jordan, J. Courtial, L. Thomson, G. Gibson, K. Karunwi, J. Cooper, Z. J. Laczik, and M. Padgett, "Interactive approach to optical tweezers control," Appl. Opt. **45**, 897–903 (2006).
7. I. Perch-Nielsen, P. Rodrigo, and J. Glückstad, "Real-time interactive 3D manipulation of particles viewed in two orthogonal observation planes," Opt. Express **13**, 2852–2857 (2005).
8. K. Svoboda, C. Schmidt, B. Schnapp, and S. Block, "Direct observation of Kinesin stepping by optical trapping interferometry," Nature **365**, 721–727 (1993).
9. O. Otto, C. Gutsche, F. Kremer, and U. F. Keyser, "Optical tweezers with 2.5 kHz bandwidth video detection for single-colloid electrophoresis," Rev. Sci. Instrum. **79**, 023710 (2008).
10. G. M. Gibson, J. Leach, S. Keen, A. J. Wright, and M. J. Padgett, "Measuring the accuracy of particle position and force in optical tweezers using high-speed video microscopy," Opt. Express **16**, 14561–14570 (2008).
11. A. Ashkin, "Forces of a single-beam gradient laser trap on a dielectric sphere in the ray optics regime," Biophys. J. **61**, 569–582 (1992).
12. A. T. O'Neil and M. J. Padgett, "Axial and lateral trapping efficiency of Laguerre-Gaussian modes in inverted optical tweezers," Opt. Commun. **193**, 45–50 (2001).

#125228 - $15.00 USD Received 9 Mar 2010; revised 11 May 2010; accepted 17 May 2010; published 19 May 2010

13. M. Speidel, L. Friedrich, and A. Rohrbach, "Interferometric 3D tracking of several particles in a scanning laser focus." Opt. Express **17**, 1003–1015 (2009).
14. A. Rohrbach, C. Tischer, D. Neumayer, E. Florin, and E. Stelzer, "Trapping and tracking a local probe with a photonic force microscope," Rev. Sci. Instrum. **75**, 2197–2210 (2004).
15. S. J. Lee and S. Kim, "Advanced particle-based velocimetry techniques for microscale flows," Microfluid. Nanofluid. **6**, 577–588 (2009).
16. J. C. Crocker and D. G. Grier, "Methods of Digital Video Microscopy for Colloidal Studies," J. Colloid. Interf. Sci. **179**, 298–310 (1996).
17. Z. Zhang and C.-H. Menq, "Three-dimensional particle tracking with subnanometer resolution using off-focus images," Appl. Opt. **47**, 2361–2370 (2008).
18. F. C. Cheong, B. Sun, R. Dreyfus, J. Amato-Grill, K. Xiao, L. Dixon, and D. G. Grier, "Flow visualization and flow cytometry with holographic video microscopy," Opt. Express **17**, 13071–13079 (2009).
19. J. S. Dam, I. R. Perch-Nielsen, D. Palima, and J. Glückstad, "Three-dimensional imaging in three-dimensional optical multi-beam micromanipulation," Opt. Express **16**, 7244–7250 (2008).
20. J. S. Dam, I. Perch-Nielsen, D. Palima, and J. Glückstad, "Multi-particle three-dimensional coordinate estimation in real-time optical manipulation," J. Europ. Opt. Soc. Rap. Public. **4**, 09045 (2009).
21. S. R. P. Pavani and R. Piestun, "Three dimensional tracking of fluorescent microparticles using a photon-limited double-helix response system," Opt. Express **16**, 22048–22057 (2008).
22. S. R. P. Pavani, A. Greengard, and R. Piestun, "Three-dimensional localization with nanometer accuracy using a detector-limited double-helix point spread function system," Appl. Phys. Lett. **95**, 021103 (2009).
23. C. Pacoret, R. Bowman, G. Gibson, S. Haliyo, D. Carberry, A. Bergander, S. Regnier, and M. Padgett, "Touching the microworld with force-feedback optical tweezers," Opt. Express **17**, 10259–10264 (2009).
24. D. Preece, R. Bowman, A. Linnenberger, G. Gibson, S. Serati, and M. Padgett, "Increasing trap stiffness with position clamping in holographic optical tweezers," Opt. Express **17**, 22718–22725 (2009).
25. W. Singer, S. Bernet, N. Hecker, and M. Ritsch-Marte, "Three-dimensional force calibration of optical tweezers," J. Mod. Opt. **47**, 2921–2931 (2000).
26. J. Leach, M. R. Dennis, J. Courtial, and M. Padgett, "Vortex knots in light," N. J. Phys. **7**, 55 (2005).
27. L. Ikin, D. M. Carberry, G. Gibson, M. Padgett, and M. J. Miles, "Assembly and force measurement with SPM-like probes in holographic optical tweezers," N. J. Phys. **11**, 023012 (2009).
28. P. J. Rodrigo, L. Gammelgaard, P. Bøggild, I. Perch-Nielsen, and J. Glückstad, "Actuation of microfabricated tools using multiple GPC-based counterpropagating-beam traps," Opt. Express **13**, 6899–6904 (2005).
29. T. Cizmar, V. Kollarova, X. Tsampoula, F. Gunn-Moore, W. Sibbett, Z. Bouchal, and K. Dholakia, "Generation of multiple Bessel beams for a biophotonics workstation," Opt. Express **16**, 14024–14035 (2008).
30. E. McLeod and C. B. Arnold, "Subwavelength direct-write nanopatterning using optically trapped microspheres," Nat. Nanotechnol. **3**, 413–417 (2008).
31. P. Galajda and P. Ormos, "Complex micromachines produced and driven by light," Appl. Phys. Lett. **78**, 249–251 (2001).
32. T. Asavei, T. A. Nieminen, N. R. Heckenberg, and H. Rubinsztein-Dunlop, "Fabrication of microstructures for optically driven micromachines using two-photon photopolymerization of UV curing resins," J. Opt. A **11**, 034001 (2009).

1. Introduction

"Optical Tweezers" is a well-established technique where small dielectric particles are confined and manipulated with a tightly focussed laser beam [1]. Holographic Optical Tweezers (HOT) [2, 3] and some counterpropagating-beam tweezers [4] extend this by allowing multiple laser foci to be produced in arbitrary 3D configurations [5] and manipulated interactively [6, 7]. Force measurement is one of the most useful capabilities of optical tweezers, and can be achieved by tracking the displacement of the trapped object from the laser focus with a quadrant photodiode [8] or a camera [9, 10].

Typically, each trap is formed as a diffraction-limited spot in the sample plane, where the microscope objective's back aperture is completely illuminated with a Gaussian or flat-top beam. However, by changing the illumination profile, we would expect to be able to alter the stiffness in the lateral and axial directions. This was first discussed by Ashkin [11] in the context of a ray optical model, where he noted that rays from the edges of the microscope aperture contribute more to the trap's axial stiffness (and less to its radial stiffness) than those in the centre. This means that a flat-top beam has a higher axial stiffness than a Gaussian beam of the same power, and that decreasing the numerical aperture (i.e. using only the centre of the back aperture) de-

#125228 - $15.00 USD Received 9 Mar 2010; revised 11 May 2010; accepted 17 May 2010; published 19 May 2010

creases the axial stiffness relative to the lateral stiffness. The use of Laguerre-Gaussian beams to enhance axial stiffness agrees with this ray-optical model [12], however more general control is possible by controlling the radial intensity profile at the back aperture.

2. 3D Position Measurement

Traditionally, particles held in optical tweezers have been tracked using a quadrant photodiode (QPD), most commonly placed in the back focal plane of the microscope condenser. This allows very precise tracking of the particle's motion in three dimensions [13]. However, this method often uses the same laser for trapping and tracking and is badly affected by changing the beam shape. It is also possible to use a weak tracking laser [14], at a different wavelength, aligned with the trapping beam. We have opted for a simpler approach based on tracking the particle with a high speed camera. This has the advantage of simple calibration and works with multiple particles simultaneously. It also has good linearity over most of its range, which is much larger than that available with QPD detection. Other 3D tracking methods have used the point spread function [15, 16], contrast inversion [17] or digital holography [18]. These techniques obtain good resolution, at the expense of relatively demanding image analysis.

Stereomicroscopy uses a modified microscope to generate two images of the sample from different viewpoints. As an object moves axially in the sample, it appears to be displaced laterally in the two images, by the same distance but in opposite directions. The axial position can therefore be found by tracking an object in 2D in each image and measuring the apparent difference in position. Commercial stereomicroscopes are designed with small angles (around 10°) between viewpoints, and as such achieve relatively coarse axial resolution [15]. It is also possible to use two separate microscope objectives [7], however this results in a large optical system and requires special sample cells.

Dam et. al. [19, 20] used structured illumination from a digital projector to obtain a stereoscopic pair of images in a tweezers system with a counterpropagating trap geometry. Left and right stereo images were separated using a colour camera, again with a relatively small separation angle. Our technique applies to single-beam optical tweezers using a single high-NA microscope objective. We use a Fourier-domain optical filter to separate the images as shown in Fig. 1, which yields much higher axial resolution due to the larger separation angle. The Fourier filter does not depend on colour to separate the left and right images, which opens the possibility of using non-brightfield imaging modes, such as fluorescence, to track particles. By using a Spatial Light Modulator (SLM) in this plane, one can create more complex Point Spread Functions (PSFs), such as a double helix [21, 22]. These images can be simply analysed to provide 3D position, though the SLM can decrease the optical efficiency of the system.

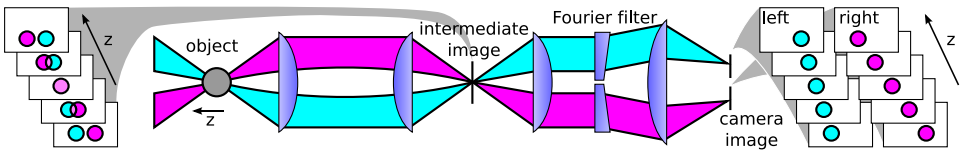

Fig. 1. Outline of the imaging system used to produce stereo images. Structured illumination produces an intermediate image with a two-lobed point spread function. Re-imaging via a Fourier filter splits this into two views from different angles.

3. Optical System

We use an inverted microscope arrangement with a high-NA objective lens (Zeiss Plan Neofluar, oil immersion, x100, NA 1.3) to image the sample onto an aperture, and then re-image onto a

#125228 - $15.00 USD Received 9 Mar 2010; revised 11 May 2010; accepted 17 May 2010; published 19 May 2010

camera (Prosilica GC640M) via a Fourier domain filter to separate the image into a stereo pair. A holographic optical tweezers system is coupled in just after the first aperture with a dichroic mirror. An expanded laser beam illuminates the SLM (Holoeye LC-R 720), which is re-imaged onto the back aperture of the objective.

The high-NA structured illumination is achieved using two short lengths of acrylic light-pipe fibres (1.5 mm diameter), illuminated by white LEDs as shown in Fig. 2(a). The fibres are placed directly above the sample without a condenser lens at a working distance of about 1.5mm, enough to illuminate through a standard microscope slide. A drop of water between the fibres and the microscope slide efficiently couples light into the system, particularly when the angle between the fibres is large. This produces an image at the focal point of the tube lens with a two-lobed point spread function, i.e. out-of-focus objects have two images, with a separation which is linearly proportional to their depth in the sample as shown in Fig. 2(b). The two images converge for in-focus objects.

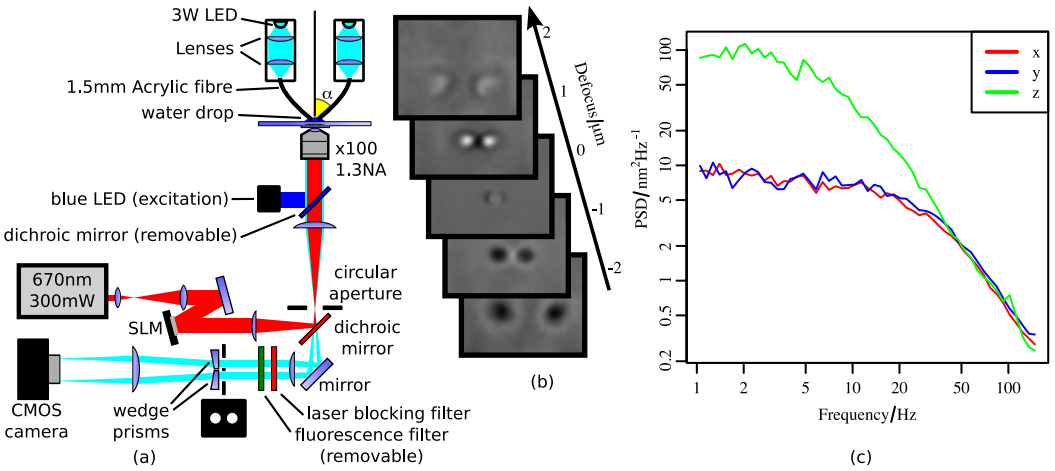

Fig. 2. (a) The optical system used for stereoscopic imaging in optical tweezers. (b) Images of a 2 μm bead at different depths, without the prisms to separate the images. (c) 3D power spectrum of a 2 μm bead's position fluctuations.

Re-imaging the back focal plane of the microscope objective shows two bright spots, one from each fibre. This corresponds to the Fourier transform of the PSF of the system. A filter consisting of two apertures and corresponding wedge prisms in this Fourier plane separates the light, forming two separate images on the camera. Thus, the lateral position of a particle can be determined simply as the average position in the two images, while the axial displacement is proportional to the difference in the x positions.

For stereoscopic imaging, the only image analysis required is tracking objects in 2D, which can be achieved to sub-pixel accuracy at up to several kHz [10], enabling the measurement of power spectra and the use of this technique in closed-loop systems [23, 24]. We fit to the marginal distributions of an image to determine the x and y positions of the bead with sub-pixel accuracy. As it is only the difference in x separation of the images which changes as the bead moves axially, we would expect $y_1 - y_2 = 0$. Noise in the tracking system means that $\langle (y_1 - y_2)^2 \rangle = 2\varepsilon^2$, where ε is the error on one measurement, typically $2-3$ nm. This is using a 2.9 ms exposure and a 340 Hz frame rate on the camera, so the spectral noise density is approximately $0.17\,\mathrm{nm\,Hz^{-1/2}}$. This yields an error of $\varepsilon/\sqrt{2} \approx 2$ nm laterally and 3 nm axially. The axial range is around $5-10\,\mu$m, depending on the effective NA of the two images (i.e. the size of the apertures in the Fourier plane and the size of the illuminating fibres).

#125228 - $15.00 USD Received 9 Mar 2010; revised 11 May 2010; accepted 17 May 2010; published 19 May 2010

Figure 2(c) shows the power spectral density of a trapped 2 μm bead's motion in x, y and z. The exposure time of our camera is approximately equal to the sampling interval, which acts as a nearly-perfect anti-aliasing filter. Thus we see the expected Lorentzian shape for all three dimensions, with a lower knee frequency in z due to the lower axial stiffness.

4. Trap Shaping

The point spread function of even a high-NA objective lens is longer axially than it is wide. This results in a lower trap stiffness in the axial direction [25], as seen in Fig. 2(c). In water, far from the coverslip, viscosity is isotropic. This means the power spectra should overlap at high frequencies, which can determine the scaling from separation to depth. We can also calculate the convergence angle using geometric optics, starting from the separation between the apertures in the Fourier plane. The two methods agree on $\alpha \approx 36^\circ$, where α is the angle between each viewpoint and the optical axis.

Different parts of the back aperture of the objective correspond to rays entering the focus from different directions, which we expect will contribute differently to the stiffness of the optical trap. We measure this by using the SLM to synthesize different apertures in the back focal plane by redirecting some of the light to the zero-order undiffracted spot [26]. The apertures used here are either simple circular apertures (which effectively reduce the NA of the trap) or annular apertures, which block out the central region as shown on the x axis of Fig. 3(a).

For each of these apertures, we use the equipartition theorem applied to the particle's position fluctuations to estimate stiffness as $k = k_b T / \langle x^2 \rangle$. This was measured over intervals of 1.5 seconds and averaged over 10-20 intervals. The resultant stiffnesses in x, y and z are plotted in Fig. 3. Data shown here has been normalised by the power in the optical trap, so the curve represents stiffness per unit optical power in the trap [an un-normalised plot is shown in Fig. 3(b)]. It is possible to create multiple traps with different apertures, as shown in Fig. 3(c), where three beads are trapped with different axial stiffness. If the trap configuration includes some traps with high axial stiffness and some with low axial stiffness, it is possible to make use of the whole back aperture and create the traps with high optical efficiency.

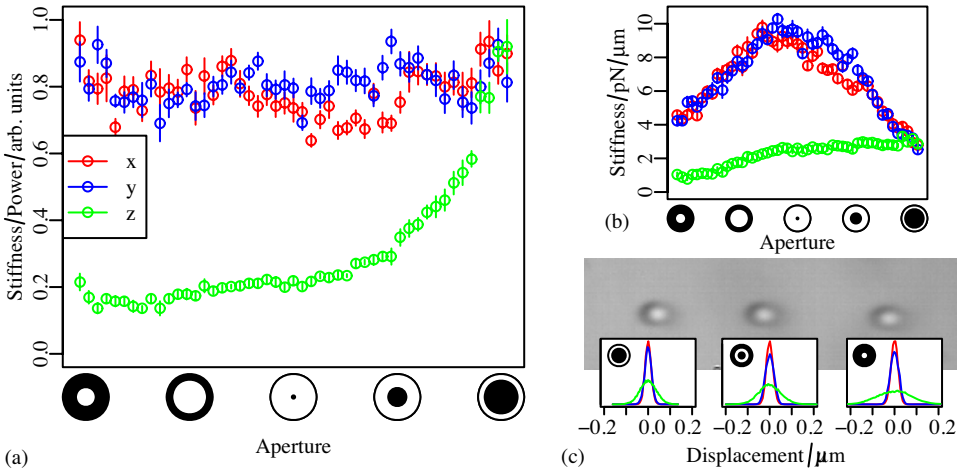

Fig. 3. (a) Stiffness of an optical trap for a 5 μm Silica bead created with various apertures at the back focal plane of the microscope objective. The values of stiffness are per unit power in the trap. (b) The same stiffnesses for fixed illumination power. (c) Position histograms for three beads trapped with different apertures, showing different axial stiffnesses.

#125228 - $15.00 USD Received 9 Mar 2010; revised 11 May 2010; accepted 17 May 2010; published 19 May 2010

This procedure was repeated for beads with a number of different sizes and materials. Figure 4 shows results for 2 μm and 3 μm diameter silica beads and for 5 μm polystyrene, where the same trends are visible. For the low-NA traps (left side of the graph), the axial stiffness is much lower than the radial stiffness. In this regime, the scattering force becomes more prominent, resulting in a shift of the equilibrium trapping position to further behind the focus. When ring-shaped traps are used, the axial stiffness starts to approach the radial stiffness. The scattering force has a smaller influence here relative to the gradient force, resulting in the bead's equilibrium position being closer to the focus.

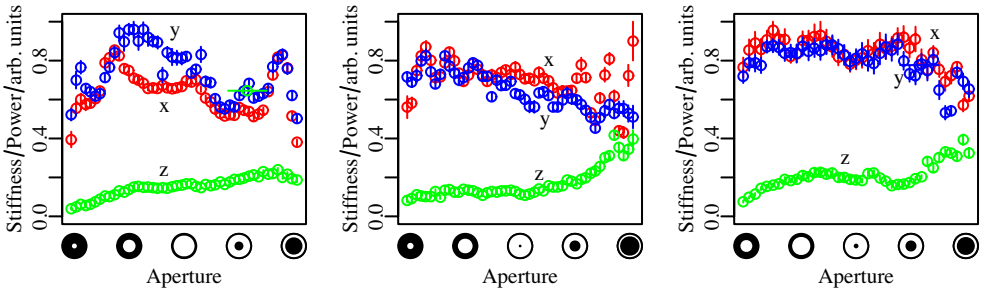

Fig. 4. Stiffness of an optical trap with various apertures, for (a) a 2 μm silica particle, (b) a 3 μm silica particle, (b) 5 μm polystyrene particle.

5. Discussion

By controlling the intensity distribution at the back aperture, we can vary k_z from nearly 0 to almost the same as the radial stiffness. This can be applied to the use of optically controlled tools and probes [27, 28], for example if a one-dimensional force measurement is to be made, the trap could be made less stiff along the direction of force measurement. Similarly, when axial force must be applied to an object, a shaped trap would allow this to be done with less light used per unit force required. Traps with a small effective NA also have a larger scattering force relative to the axial stiffness, which is weak due to the extended axial PSF. This is a property shared by Bessel Beams [29], recently exploited to hold beads just above a surface for UV nanopatterning [30]. Using an SLM to shape the trap means that we can alter the characteristics of a trap dynamically and we are able to have multiple traps, each with a different shape. When using light to power micro-machines, for example [31, 32], it can be advantageous to have some traps with high axial stiffness and some which are dominated by the scattering force (i.e. very low axial stiffness). If both shapes of trap are required, this can be done with very good efficiency.

6. Conclusions

We have demonstrated that Holographic Optical Tweezers can be used to change the shape of individual traps, resulting in different stiffnesses for different directions. This allows us to provide, for example, a higher ratio of axial to lateral stiffness or a very weak trap in one dimension. This can be performed independently on several traps at the same time, which is a useful ability when working with tools or optically driven micro-machines. Particle tracking in a stereoscopic microscope with extremely high separation between the two viewpoints was used to establish the changes in trap stiffness observed. This enables accurate, linear tracking of axial position using only simple 2D particle tracking algorithms. This could easily be extended to track non-spherical objects which are very difficult to track using most other methods.

#125228 - $15.00 USD Received 9 Mar 2010; revised 11 May 2010; accepted 17 May 2010; published 19 May 2010